1-1-1993

Contributions of the low-latitude boundary layer to the finite width magnetotail convection model

Harlan E. Spence
Boston University, harlan.spence@unh.edu

M. G. Kivelson

Recommended Citation

Spence, H. E., and M. G. Kivelson (1993), Contributions of the low-latitude boundary layer to the finite width magnetotail convection model, J. Geophys. Res., 98(A9), 15487–15496, doi:10.1029/93JA01531.

JOURNAL OF GEOPHYSICAL RESEARCH, VOL. 98, NO. A9, PAGES 15,487–15,496, SEPTEMBER 1, 1993

Contributions of the Low-Latitude Boundary Layer to the Finite Width Magnetotail Convection Model

HARLAN E. SPENCE

Space and Environment Technology Center, The Aerospace Corporation, Los Angeles, California

MARGARET G. KIVELSON

Department of Earth and Space Sciences and Institute of Geophysics and Space Physics, University of California, Los Angeles

Convection of plasma within the terrestrial nightside plasma sheet contributes to the structure and, possibly, the dynamical evolution of the magnetotail. In order to characterize the steady state convection process, we have extended the finite tail width model of magnetotail plasma sheet convection. The model assumes uniform plasma sources and accounts for both the duskward gradient/curvature drift and the earthward $\mathbf{E} \times \mathbf{B}$ drift of ions in a two-dimensional magnetic geometry. During periods of slow convection (i.e., when the cross-tail electric potential energy is small relative to the source plasma's thermal energy), there is a significant net duskward displacement of the pressure-bearing ions. The electrons are assumed to be cold, and we argue that this assumption is appropriate for plasma sheet parameters. We generalize solutions previously obtained along the midnight meridian to describe the variation of the plasma pressure and number density across the width of the tail. For a uniform deep-tail source of particles, the plasma pressure and number density are unrealistically low along the near-tail dawn flank. We therefore add a secondary source of plasma originating from the dawnside low-latitude boundary layer (LLBL). The dual plasma sources contribute to the plasma pressure and number density throughout the magnetic equatorial plane. Model results indicate that the LLBL may be a significant source of near-tail central plasma sheet plasma during periods of weak convection. The model predicts a cross-tail pressure gradient from dawn to dusk in the near magnetotail. We suggest that the plasma pressure gradient is balanced in part by an oppositely directed magnetic pressure gradient for which there is observational evidence. Finally, the pressure to number density ratio is used to define the plasma "temperature." We stress that such quantities as temperature and polytropic index must be interpreted with care as they lose their nominal physical significance in regions where the two-source plasmas intermix appreciably and the distributions become non-Maxwellian.

1. INTRODUCTION

Recently, there has been renewed interest in describing the large-scale flow of mass, momentum, and energy within the terrestrial magnetotail. The description of particle transport in the tail is fundamental; it is crucial to our understanding of the convective stability of the magnetotail as well as to its structure, both in space and time. Although it is becoming increasingly clear that bursty flows are present even during relatively quiet times [*Baumjohann and Paschmann*, 1989; *Angelopoulos et al.*, 1992, 1993], the steady state convection problem remains relevant both to characterize the time-averaged plasma sheet and to provide a standard against which the contribution of dynamic flows can be compared.

The magnetotail convection problem has been approached using a variety of techniques. Studies of the convective motion of magnetotail plasma sheet plasma have included global MHD simulations [*Walker and Ogino*, 1989], theoretical models [*Kivelson and Spence*, 1988; *Hau et al.*, 1989; *Kan and Baumjohann*, 1990; *Pontius and Wolf*, 1990; *Pritchett and Coroniti*, 1990; *Spence and Kivelson*, 1990; *Erickson et al.*, 1991; *Goertz and Baumjohann*, 1991; *Ashour-Abdalla et al.*, 1992; *Kan et al.*, 1992] and statistical data surveys [*Baumjohann and Paschmann*, 1989; *Huang et al.*, 1989; *Zhu*, 1990]. In this paper, we report on new results obtained from the finite tail width convection model discussed previously by *Kivelson and Spence* [1988] and *Spence and Kivelson* [1990] (hereinafter referred to as KS88 and SK90, respectively).

The finite tail width convection model is an extension of the original analysis of *Erickson* [1985]. The underlying premise of the model is that as hot particles convect earthward under the influence of $\mathbf{E} \times \mathbf{B}$ motion, they also gradient and curvature drift across the tail in time stationary fields. If an electric potential is applied across the tail, a flux tube loaded with plasma in the deep magnetotail drifts earthward with an energy-independent convective velocity. However, energy-dependent gradient/curvature drifts cause the plasma on the initial flux tube to "smear" and the flux tube loses its integrity. The effect is unimportant in a tail of very large width but becomes manifest in a tail of finite width when the cross-tail distance is comparable to the distance of plasma displacement along the tail axis. In this limit, the bulk properties of the convected plasma are significantly different from those obtained by invoking simple adiabatic compression of a relatively cold plasma population. In particular, the pressure [KS88] and number density [SK90] along the midnight meridian can be lowered substantially relative to values obtained using PV^{γ} = const. and nV = const.

Paper number 93JA01531.
0148-0227/93/93JA-01531$05.00

The goals of this paper are to address two limitations of the previously reported finite tail width convection model and to model more fully the characteristics of the inner plasma sheet. Previous accounts of the finite tail width models described bulk plasma parameter variations only along the midnight meridian. Herein we solve for the number density and pressure in the magnetospheric equatorial plane across the full width of the tail. Our preliminary results considered only a deep-tail source of plasma sheet plasma. In this paper, we add the low-latitude boundary layer (LLBL) as an additional plasma source. We present results from the revised model and show that the LLBL plasma source is important in parts of the near tail under certain conditions. We also present several predictions pertaining to the large-scale structure of the inner plasma sheet that may be testable through observation. Finally, we justify and/or assess the impact of several simplifying model assumptions.

2. Model Description

In this section we describe the finite tail width model briefly and identify the pertinent assumptions. We shall use geocentric solar magnetospheric (GSM) coordinates and, for simplicity, consider a two-dimensional magnetotail configuration consistent with a zero dipole tilt condition and low levels of geomagnetic activity. We assume that at some large down-tail distance the magnetotail field and plasma properties approach an asymptotic limit [see *Birn*, 1987]. We take this distance to be $x = -60R_E$ and assume as one model boundary condition that tail plasma is distributed uniformly with cross-tail (y) location. Figure 1 illustrates schematically the model geometry. Data surveys have shown that ions carry the bulk of the energy density in the magnetotail plasma sheet [*Spence et al.*, 1989; *Baumjohann and Paschmann*, 1989] and that protons are normally the dominant ion species. As we are interested in determining the bulk thermal properties of the plasma sheet plasma, we consider the electrons to be cold and the ions to be protons. In the concluding remarks, we show that neglect of electron pressure is a good approximation. The tail source (identified by subscript "T") proton distribution is assumed to be Maxwellian, characterized by a temperature T_T, and a number density n_T. We assume that the plasma in the dawnside LLBL (identified by subscript "L") is uniform with down-tail distance and is characterized by number density n_L, and Maxwellian temperature T_L. In our model, the dawnside LLBL plasma source extends from $-60 < x < -10R_E$ and lies at the nonflaring tail boundary at $y = -18R_E$. We do not concern ourselves with the LLBL at the dusk boundary of our model as it does not contribute ions to the central magnetotail through the gradient/curvature drift mechanism.

Earthward $\mathbf{E} \times \mathbf{B}$ convection of the plasma is driven by a uniform magnetotail electric field, $\mathbf{E}$, pointing from dawn to dusk across a nonflaring tail of width $2R$, where $R = 18R_E$. The assumption of a uniform cross-tail electric field is a first-order, simplifying approximation; fully self-consistent electric fields (i.e., those including x-directed components) may modify these results substantially in certain regions and these implications are discussed in a later section. We assume a two-dimensional magnetic field configuration, uniform across the tail, and use the magnetic field given by the midnight meridian cut through the $Kp = 0, 0^+$ *Tsyganenko* [1987] (hereinafter referred to as T87) model (see his Figure 2). We assume that pitch angle scattering maintains isotropic distributions and that loss of particles along flux tubes is negligible. The latter assumption is justified, for instance, by the work of *Southwood and Wolf* [1978], who argued that convective time scales are much shorter than the strong pitch angle diffusion time scale.

Liouville's theorem specifies the mapping of the phase space distribution function from the source (LLBL and tail) to other locations. Bounce-averaged drift theory is used to describe the magnetic equatorial trajectory of bounce orbits. Shells of phase space with different energies are followed independently for the two source populations. Protons from a portion of phase space with thermal speed v_i, drifting slowly on a flux tube with a volume per unit magnetic flux, V_i, must satisfy

$$v_f{}^2 = v_i{}^2 \left(\frac{V_i}{V_f} \right)^{2/3} \tag{1}$$

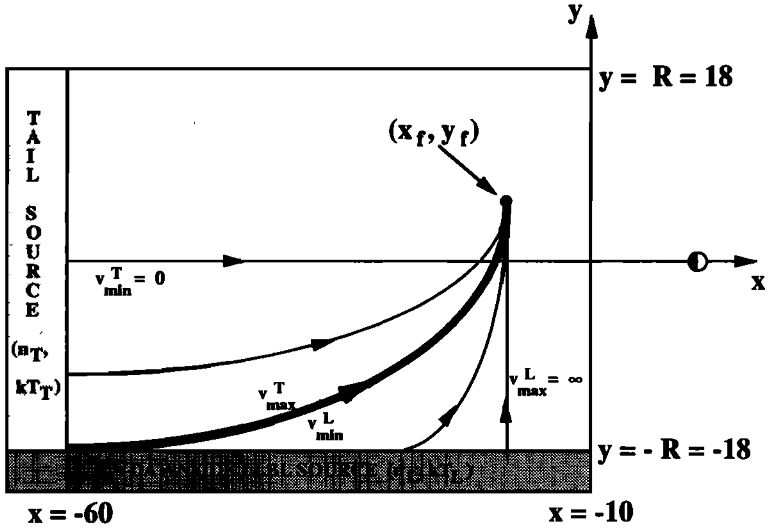

Fig. 1. Schematic illustrating the magnetotail geometry and the dual sources of plasma used in the finite tail width convection model.

Here v_f is the thermal speed at the final position where V_f is the corresponding flux tube volume. The volume per unit magnetic flux is given by

$$V = \int \frac{ds}{B} \tag{2}$$

where ds is the differential element along the magnetic field and where the integration is taken from the northern to the southern ionosphere. Conservation of energy requires that

$$-qEy_f + \frac{1}{2}mv_f{}^2 = -qEy_i + \frac{1}{2}mv_i{}^2 \tag{3}$$

where y_f (y_i) is the final (initial) cross-tail location.

Pressure and number density are obtained from velocity moments of the local particle distribution function; the finite width of the tail imposes finite limits on the velocity integrals. Particles that can reach an arbitrary location (x_f, y_f) earthward of the tail source with the highest thermal speed start at the dawnside, deep-tail boundary, so we set $y_i = -R$. We evaluate (3) to find that at the deep-tail source, these particles have a thermal energy,

$$\frac{1}{2}mv_{T,\max}{}^2 = \frac{qE(R+y_f)}{(V_i/V_f)^{2/3}-1} \tag{4}$$

where V_i is the flux tube volume at the tail boundary at $x_i = -60$. Owing to their relatively large gradient/curvature drift, tail source particles with initial thermal speeds greater than $v_{T,\max}$ are swept duskward, antisunward of the target location.

Whereas the deep-tail particle access is limited by an upper velocity bound, the LLBL particle access is limited by a lower velocity bound. Dawnside LLBL particles with sufficiently high energy have ready access to the near-tail central plasma sheet at any y location because their cross-tail gradient/curvature drift is rapid relative to sunward $\mathbf{E}\times\mathbf{B}$ drift. Conversely, the motion of LLBL source particles with very low energy is dominated by earthward $\mathbf{E}\times\mathbf{B}$ drift, and they may not drift from dawn-to-dusk rapidly enough to access locations far from the dawnside tail flank. It follows then that at position (x_f, y_f) in the inner central plasma sheet, particles from the LLBL source have the minimum energy if they convect from the most distant down-tail LLBL at $x_i = -60, y_i = -18$. At this source location, their initial thermal speed $v_{L,\min}$ must satisfy (3), from which it follows that

$$\frac{1}{2}mv_{L,\min}{}^2 = \frac{qE(R+y_f)}{(V_i/V_f)^{2/3}-1} \tag{5}$$

The pressure and number density contributed by the tail plasma source follow directly from the midnight meridian solutions discussed in KS88 and SK90, with the replacement, $R \rightarrow R + y_f$. Only the upper velocity limit on the integrals over phase space changes as a function of cross-tail position; the form of the integral remains unchanged. Therefore the generalized number density and pressure ratios contributed by the tail source may be expressed as before

$$\frac{n(x_f,y_f)}{n_\infty(x_f,y_f)} = \mathrm{erf}(\xi_T) - \frac{2\xi_T}{\sqrt{\pi}}e^{-\xi_T{}^2} \tag{6}$$

$$\frac{P(x_f,y_f)}{P_\infty(x_f,y_f)} = \mathrm{erf}(\xi_T) - \frac{2\xi_T}{3\sqrt{\pi}}e^{-\xi_T{}^2}(3+2\xi_T{}^2) \tag{7}$$

where erf is the error function, and

$$\xi_T{}^2 = \frac{r_T}{\left[V_i(x_i)/V_f(x_f)\right]^{2/3}-1} \tag{8}$$

$$r_T = \frac{qE(R+y_f)}{kT_T} \tag{9}$$

The number density (pressure) is normalized by n_∞ (P_∞) which is the value obtained by assuming strictly lossless, time-independent, adiabatic convection; i.e., $n_\infty \propto V^{-1}$ ($P_\infty \propto V^{-5/3}$). The y dependence of the solutions enters explicitly in the parameter r_T. As before, the x dependence enters through the flux tube volume.

In a manner analogous to that for the tail plasma, (1) may be used to relate the minimum velocity in the LLBL source distribution to $v_{L;f,\min}$, the minimum velocity at some final location. At position (x_f, y_f), the number density contributed by the LLBL plasma source is given by

$$n(x_f,y_f) = 4\pi\int_{v_{L;f,\min}}^{\infty} v^2 f\left[v(x_f,y_f)\right]dv \tag{10}$$

or

$$\frac{n(x_f,y_f)}{n_L} = e^{r_L}\left[\frac{2}{\sqrt{\pi}}\xi_L e^{-\xi_L{}^2} + \mathrm{erfc}(\xi_L)\right] \tag{11}$$

where

$$\xi_L{}^2 = \frac{r_L}{1-\left[V_f(x_f)/V_i(x_i)\right]^{2/3}} \tag{12}$$

$$r_L = \frac{qE(R+y_f)}{kT_L} \tag{13}$$

and erfc(t) is the complementary error function [erfc(t) = 1−erf(t)]. The second velocity moment of the phase space distribution function gives

$$P(x_f,y_f) = \frac{4\pi m}{3}\int_{v_{L;f,\min}}^{\infty} v^4 f\left[v(x_f,y_f)\right]dv \tag{14}$$

or

$$\frac{P(x_f,y_f)}{P_L} = e^{r_L}\left[\frac{2\xi_L}{\sqrt{\pi}}e^{-\xi_L{}^2}(1+\frac{2}{3}\xi_L{}^2) + \mathrm{erfc}(\xi_L)\right] \tag{15}$$

In summary, (6) and (7), and (11) and (15) describe the number density and pressure, at an arbitrary location in the equatorial plane, contributed by the tail and LLBL plasma sources, respectively.

Before presenting results of this formulation, it is important to point out that the effects of corotation have been neglected. The corotation drift acts in the direction opposite to the ion gradient-B drift and may become important near the very inner edge of our model ($-15 < x < -10$). By mapping the corotation potential at the Earth's surface along assumed equipotential T87 magnetic field lines to the magnetospheric equator we find that the corotation speed at midnight in the near-tail is < 5 km/s. The gradient-B drift is energy-dependent. Between x = -10 and -15, the gradient-B drift of 300-eV protons is approximately 5 km/s. Thus corotation dominates the motion of protons with energies less than or equal to approximately 300 eV within the near-tail region near midnight. (We find that away from midnight [$|y| > 5$ R_E], the corotation velocity y component decreases owing to the geometry of the full, three-dimensional magnetic field. This lowers the energy at which corotation dominates.) On the other hand, the important pressure-bearing particles from the tail source that are "lost" owing to the gradient-B effect have energies greater than approximately 2.5 keV. At these higher energies, the gradient-B drift speeds are approximately 10 times greater than the corotation speed. Consequently, corotation is important in our model only for those tail particles that have ready access to the inner magnetotail (i.e., those for which gradient-B effects are minimal), and we may ignore, to first-order, the complications associated with adding self-consistently the corotation field. Similar corotation effect arguments apply also to the LLBL source particles. Those pressure-bearing LLBL particles that have access to the inner magnetotail near midnight (i.e., with energies exceeding the minimum cutoff energy of approximately 2.5 keV) are likewise little affected by corotation electric fields.

3. Solutions from the Two Plasma-Source Model

We present solutions of the bulk plasma moments in a common format. Figure 2 plots the plasma pressure and number density in the equatorial plane and illustrates contributions from the tail source only (Figure 2*a*), the LLBL source only (Figure 2*b*), and the combined sources (Figure 2*c*). Figure 2*d* shows contours of the percentage each source contributes to the net pressure and density. The net effective "temperature" from both sources (Figure 2*c* format) is shown later. In each case, contours of the equatorial bulk plasma moment are plotted on an x-y grid ($z = 0$) whose boundaries define approximately the geomagnetic tail region. All calculations assume that the uniform, far-tail plasma is a Maxwellian with number density $n_T = 0.1$ cm^{-3} and temperature $kT_T = 2.5$ keV, consistent with observations [see KS88 and SK90]; that the uniform LLBL plasma is a Maxwellian with number density $n_L = 0.5$ cm^{-3} and temperature $kT_L = 0.7$ keV, consistent with the typical dawnside plasma measurements reported by *Eastman et al.* [1985]; and that the cross-tail electric potential is 15 kV, appropriate to magnetically quiet conditions [*Kivelson*, 1976].

3.1. Plasma Sheet Plasma Pressure

We consider first the modeled plasma pressure shown in Figure 2. Panel *a* illustrates clearly the effect that gradient/curvature drift has on the pressure-bearing particles in the near-tail region. In the absence of gradient/curvature drift, pressure contours from the tail plasma source would

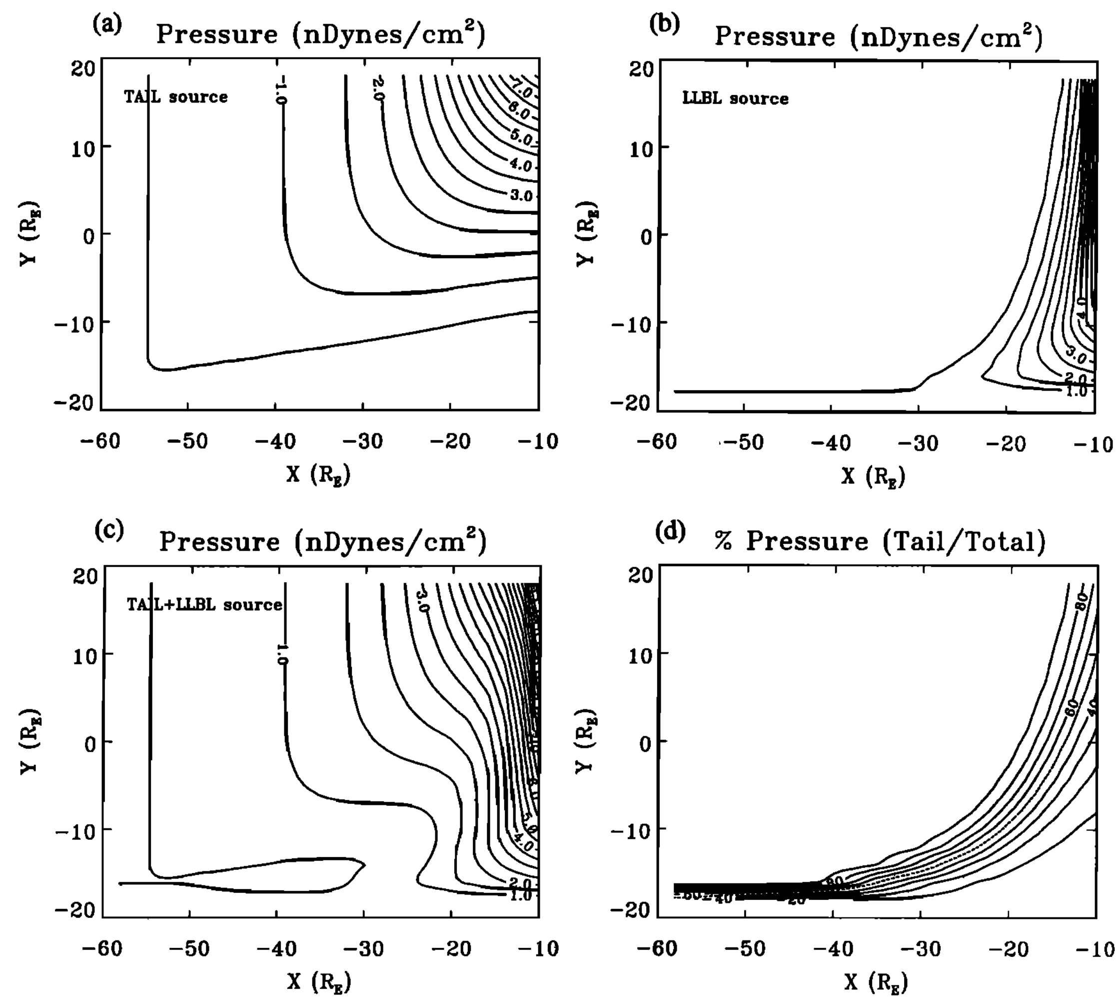

Fig. 2. Contours of the plasma pressure are shown in the magnetospheric equatorial plane (*a*) for the deep-tail source only, (*b*) for the LLBL source only, and (*c*) for the combined sources. (*d*) Contours of the percentage of plasma pressure (10% increments) contributed by the deep-tail source. The pertinent model parameters used in the calculations are $n_T = 0.1$ cm^{-3}, $kT_T = 2.5$ keV, $n_L = 0.5$ cm^{-3}, $kT_L = 0.7$ keV, $qER = 7.5$ keV.

be parallel to the y axis and the pressure gradient would point earthward. Such a situation pertains at large down-tail distances ($x < -35R_E$), where the gradient/curvature drift affects preferentially the high-energy tail of the proton distribution function that contributes little to the pressure. On the other hand, in regions where westward gradient/curvature drift of the pressure-carrying particles is large relative to their sunward $\mathbf{E} \times \mathbf{B}$ drift, the pressure gradient points predominantly dawn-to-dusk across the tail. Such a situation pertains in the near-tail region ($x > -20R_E$), where the westward drifting protons dominate the plasma pressure. The magnitude of the cross-tail pressure gradient increases earthward owing to the increasing influence of the y-directed gradient/curvature drift for particles of lower energies.

The unrealistically large cross-tail pressure gradient near the inner edge of the tail in Figure 2*a* underscores the limitations of a model in which the only source of plasma is the deep tail. Comparing Figures 2*a* and 2*b*, we note that at large down-tail distances ($x < -30R_E$), the LLBL plasma source contributes little to the equatorial plasma pressure across the tail. At these distances, the sunward $\mathbf{E} \times \mathbf{B}$ drift is dominant for the pressure-carrying LLBL particles and the pressure peaks close to the dawnside LLBL. For $x > -30R_E$, the duskward gradient/curvature drift is comparable to the sunward $\mathbf{E} \times \mathbf{B}$ drift, shifting the pressure peak away from the dawn boundary and producing a sunward pressure gradient. The LLBL plasma source is seen to be important only in the near-magnetotail. In particular, the dawnside LLBL proton source contributes to the total CPS plasma pressure for $x > -20$ and $y < 0$ R_E.

Figure 2*c* combines the partial pressure contributions from the two sources. The relative importance of the deep-tail source to the total pressure is illustrated in Figure 2*d*; the 50% demarcation location is plotted with a dotted curve. At large down-tail distances ($x < -40R_E$), where the tail is the dominant plasma source, a nearly uniform but shallow pressure gradient, positive sunward, is present. The LLBL contribution dominates at intermediate distances ($-40 < x < -25$) near the dawn tail flank, and in the postmidnight half of the near magnetotail plasma sheet ($x > -25R_E$) where it contributes > 50% of the plasma pressure.

The addition of the LLBL plasma source virtually eliminates the difference between the lobe magnetic pressure and the plasma sheet thermal pressure near the inner edge of the plasma sheet along the midnight meridian, that was an unsatisfactory feature of our previous analysis (KS88). The dotted curve of Figure 3 shows the down-tail variation of the pressure along the midnight meridian when only a deep-tail plasma source is included ($\tau_T = 3$) as in KS88; the adiabatic pressure profile (dashed-dotted curve proportional to $V^{-5/3}$) is also shown for reference. The dashed curve shows the corresponding observed tail lobe magnetic pressure variation with down-tail distance (after KS88). The observed equatorial plasma pressure curve identified in Figure 3 was obtained by fitting a four-parameter function to the average quiet time observations discussed by *Spence et al.* [1989, Figure 8]. The empirical plasma sheet pressures were then scaled upward by a constant amount in order to match the lobe magnetic pressure curve at $x = -30R_E$. (The unscaled plasma pressure curve is given by $P(x) =$

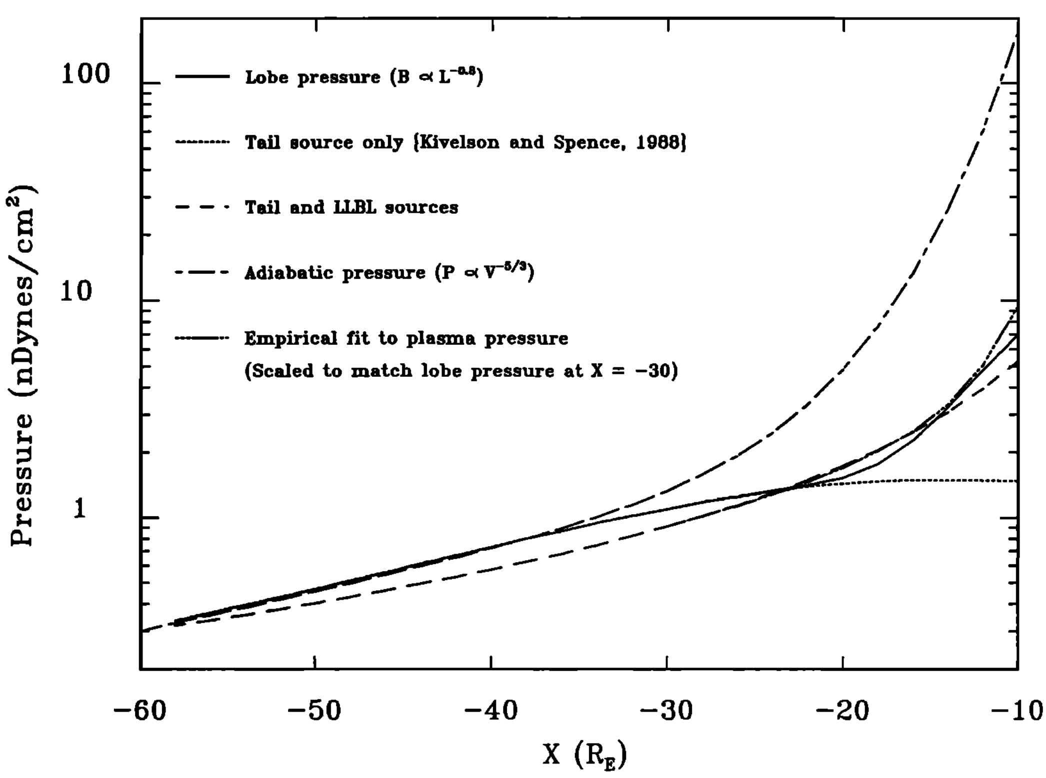

Fig. 3. Profiles of theoretical pressure along the midnight meridian with and without the LLBL plasma source. The observed lobe magnetic and plasma sheet plasma pressure curves, as well as the pressure obtained by assuming two-dimensional adiabatic compression, are shown for comparison.

$8.9 \times 10^{-7} e^{-0.59|x|} + 8.9 \times 10^{-8} |x|^{-1.53}$, where x is the distance along the Earth-Sun direction in R_E and the fitted pressure is in dynes/cm^2. The coefficients were obtained from weighted (according to the number of data points in each x bin), nonlinear least squares fit [*Bevington*, 1969] to the data; the equation is applicable between $x = -3.5 R_E$ to $\sim -30 R_E$ in the midnight meridian.) One notes that both the quiettime lobe magnetic and plasma sheet plasma pressure increase earthward without a change of inflection whereas with solely a deep-tail plasma source, the modeled plasma pressure profile follows the observed pressures from $-60 < x < -25$, changes inflection, and falls substantially below the observed pressures for $x > -25$. With the addition of a LLBL plasma source, for the same r_T, we find that the net plasma pressure curve more closely approximates the empirically determined pressure curves. The remaining differences in curvature are probably not significant considering our very simplified model. As the lobe magnetic and modeled plasma sheet plasma pressures should be nearly equal in the tail, the LLBL plasma source must be important for accurate descriptions of the inner magnetotail plasma structure during periods of slow convection.

Perhaps the most interesting feature in Figure 2c is that a large cross-tail pressure gradient in the near-tail region persists at a reduced level even when both plasma sources are considered. The average cross-tail pressure gradient within the range $-20 < x < -10 R_E$ ($\sim$ 0.2 ndynes/cm^2-R_E) is comparable to the average sunward gradient ($\sim$ 0.4 ndynes/cm^2-R_E). The cross-tail pressure gradient is steeper in the dusk half of the plasma sheet than in the dawn half and is strongly x-dependent. The average magnitude decreases to $\sim$0.02 ndynes/cm^2-R_E within the range $-40 < x < -30 R_E$ and is essentially zero for $-60 < x < -50$ R_E.

Possible evidence for a cross-tail pressure gradient has been discussed in the published literature. *Liu and Rostoker* [1991] reported on a survey of plasma measurements from ISEE 1 that revealed the presence of a dawn/dusk asymmetry in the central plasma sheet pressure. Preliminary results indicate that the plasma pressure increases toward dusk within the region sampled ($-18 < x - 10$, $-20 < y < 10$), during both quiet and moderately disturbed periods. Furthermore, the cross-tail gradient increases earthward. They report that the average cross-tail pressure gradient magnitude, calculated for $-18 < x < -13$ for quiet conditions, is $\sim$0.15 ndynes/cm^2-R_E, qualitatively consistent with our model. Recent data surveys by *Angelopoulos et al.* [1993] and *Zhu* [1993] have demonstrated that the quiet-time-averaged, background flows in the near-Earth plasma sheet have a strong dawn-to-dusk component. The sense of these cross-field flows, carried in large part by those ions that contribute significantly to the energy density of the plasma, are consistent with a cross-tail pressure gradient of the sort reported by *Liu and Rostoker* [1991]. We propose that the gradient/curvature drift mechanism explains, at least in part, this reported observed pressure asymmetry.

Having inferred a dawn-to-dusk plasma pressure gradient, one may ask whether the plasma sheet can maintain equilibrium in the presence of the gradient. In the quasistatic approximation ($\rho(\partial \mathbf{v}/\partial t) \to 0$) and for slow convection ($\rho(\mathbf{v} \cdot \nabla)\mathbf{v} \to 0$), the MHD momentum equation becomes

$$\nabla\left(P + \frac{B^2}{8\pi}\right) = \frac{1}{4\pi}(\mathbf{B} \cdot \nabla)\mathbf{B} \qquad (16)$$

if the plasma pressure is isotropic. The y component of (16) is

$$\frac{\partial}{\partial y}\left(P + \frac{B^2}{8\pi}\right) = \frac{1}{4\pi}\left(B_x \frac{\partial}{\partial x} + B_y \frac{\partial}{\partial y} + B_z \frac{\partial}{\partial z}\right)B_y \qquad (17)$$

The tail approximation [e.g., *Schindler and Birn*, 1986] allows us to take

$$B_x, \frac{\partial}{\partial z} = O(1) \qquad B_y, B_z, \frac{\partial}{\partial x}, \frac{\partial}{\partial y} = O(\epsilon) \qquad (18)$$

Then (18) reduces to the simple pressure balance equation

$$\frac{\partial}{\partial y}\left(P + \frac{B^2}{8\pi}\right) = 0 \qquad (19)$$

Equation (19) requires that the dawn-to-dusk plasma pressure gradient, should be balanced by an equal magnitude but oppositely directed magnetic pressure gradient in the tail plasma sheet. Standard empirical magnetospheric magnetic field models (including the T87 model used in this study) do not provide insight into gradients of this sort as they assume symmetry about the noon-midnight meridian. However, the work of *Fairfield* [1986] indicates that a dawn-to-dusk gradient exists. Fairfield analyzed magnetic field data from the IMP 6, 7, and 8 spacecraft when they were in the near-tail region ($-40 < x < -10 R_E$) within $\pm 3 R_E$ of the estimated location of the neutral sheet. He binned the data according to the AE index, down-tail and cross-tail location, and interplanetary magnetic field sector polarity. During magnetically quiet intervals ($AE < 50$ nT) in the near-tail ($-20 < x < -10 R_E$), Fairfield found that the average magnetic field magnitude was 17.4 nT in the dawn sector and only 7.5 nT in the dusk sector. Nearly 90% of the field magnitudes exceeded 10 nT in the dawn sector, while more than 80% were less than 10 nT in the dusk sector. Thus the average magnetic pressure in the dawn sector was $\sim$ 5.4 times that in the dusk sector. (Near midnight, the average magnitude was comparable with that found in the dawn sector; however, the distribution was quite broad relative to those in both the dawn and dusk sectors. Fairfield noted that the broad range of values near midnight may be attributed both to the relative thinness of the plasma sheet and to the relatively large radial variation of B.) It is important to note that this cross-tail, equatorial magnetic field magnitude gradient was not discernible in data obtained either at larger down-tail distances or during geomagnetically disturbed conditions. *Fairfield* [1986] speculated that the low magnetic field measured near dusk was a diamagnetic reduction caused by the net westward drift of energetic ions (the physical mechanism that is analyzed quantitatively in our model).

Plasma sheet magnetic pressure gradients have the proper signs and appropriate magnitudes to balance the plasma sheet plasma pressure gradients described by our model. Obviously, an inconsistency of the model is that the field has been taken to be uniform in y. We know, for example, that the normal component of the plasma sheet magnetic field and also the flux tube volume varies with cross-tail location, owing in part to the differential degree of tail field stretching near the center of the tail relative to that near the flanks. This geometric effect is symmetric about the noon-midnight meridian and thus does not contribute to dawn-dusk asymmetries. On the other hand, the gradient drift effect likely contributes a sizable dawn-dusk asymmetric component to the plasma sheet magnetic field. Consequently, the cross-magnetotail magnetic field gradient will contribute an earthward component to the ion gradient/curvature drift and a dependence of flux tube volume on y. Both of these effects will be relatively more important in regions of larger magnetic field strength and gradients (i.e., near the inner edge of the plasma sheet near midnight), but full analysis is beyond the scope of this paper. In addition to magnetic pressure gradients, other possible sources for the required stress balance include magnetic curvature forces (field-aligned currents) or time variations and these are discussed later.

3.2. Plasma Sheet Number Density

The modeled number densities are shown in Figure 4. As with plasma pressure, we find that during quiet times the LLBL contributes significantly to the near-tail plasma sheet number density and to the dawnside section of the magnetotail at intermediate tail distances. While the combined number density is relatively uniform across the tail for $x > -25R_E$, the phase space distribution is composed of a cold but dense component originating from the LLBL and a hot but tenuous component originating in the deep tail. The admixture of the two components varies both as a function of cross-tail and down-tail location. For example, there is predominantly a cold, dense plasma near the dawn magnetotail flank for $x > -40R_E$, but a hot plasma near dusk for $x > -20R_E$. This feature is illustrated more clearly in Figure 4*d* which plots contours of the percentage of the total number density contributed by the deep-tail plasma source.

The mixture of cold and warm plasmas should be evident in measured plasma sheet phase space distributions. We note that *Eastman et al.* [1985] analyzed plasma measurements obtained by the IMP and ISEE satellites and reported on characteristics of the magnetotail plasma sheet relevant to this point. One of the outstanding new results that they reported was that the central plasma sheet often contains both a hot and a cold ion component. The colder, denser component was consistently observed near the magnetotail flanks; the data examples presented to illustrate this feature were all from near the dawn flank. *Eastman et al.* [1985] concluded that the cold component resulted from diffusive transport of LLBL particles and suggested that the magnetotail boundary layer might be the dominant contributor of the central plasma sheet, particularly during periods of geomagnetic quiet. Our model results support their latter suggestion, although we invoke a somewhat different transport mechanism.

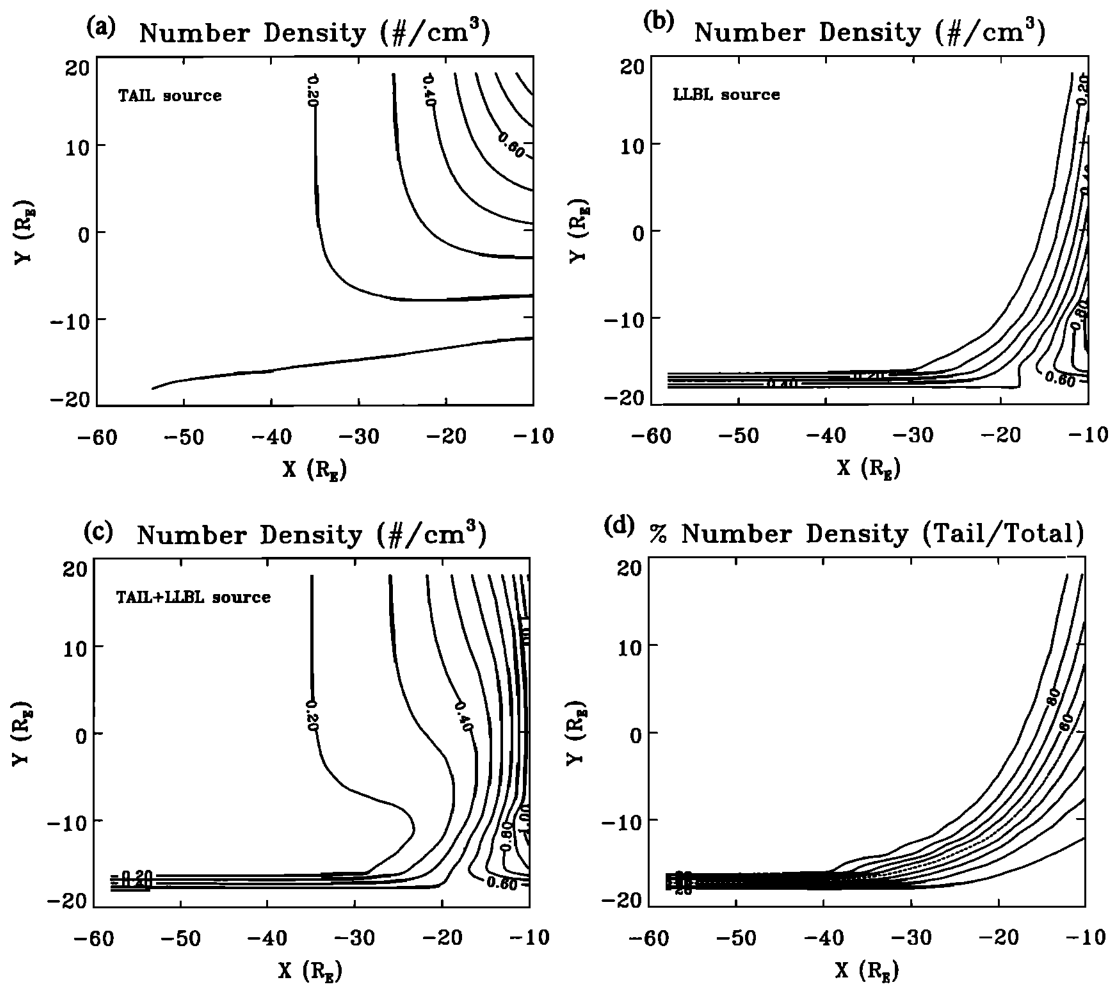

Fig. 4. Contours of the number density using the same format and parameters as in Figure 2.

3.3. *Plasma Sheet "Temperature" and Effective Polytropic Index*

The finite tail, dual-source model produces a rather strange plasma distribution in the near-tail central plasma sheet. The part of the phase space distribution mapped from the deep tail lacks particles above a critical energy while the part mapped from the LLBL lacks particles below another critical energy. The conglomerate distribution function in the inner magnetosphere may thereby become quite non-Maxwellian (in the absence of any thermalization process) during periods of slow convection; the relations among the moments of the distribution are thus affected. Strictly speaking, it is not possible to assign a temperature to such a distribution. However, an effective plasma sheet temperature (or average thermal energy) can be defined by $kT = P/n$, and that is plotted in Figure 5. As mentioned above, the dawn tail flank is relatively cool ($kT \lesssim 2$ keV) because the dominant source is the cold LLBL plasma ($kT = 0.7$ keV). In contrast, the dusk tail flank in the near-tail is considerably hotter ($kT \gtrsim 5$ keV) owing primarily to adiabatic compression of the dominant hot tail plasma ($kT = 2.5$ keV). Again, we emphasize that much of the cross-tail pressure gradient is due to this cross-tail temperature gradient, not to cross-tail variations of the number density.

The contributions of the two plasma sources to the plasma in the inner magnetotail during quiet times may produce anomalous relationships between measured plasma sheet "temperature" (or pressure) and number density [e.g., *Baumjohann and Paschmann*,1989; *Huang et al.*, 1989; *Zhu*, 1990] and lead to thermodynamically improbable constitutive relationships. In particular, the relationships change as a function of position within the plasma sheet. This point is illustrated in Figure 6 which shows the average thermal energy, pressure, and number density as a function of down-tail location in the equatorial plane at several different cross-tail locations ($y = -16, -8, 0, 16 R_E$). Let us compare the variations along the x axis at two $y =$ const. planes. Adjacent to the dawn tail flank at $y = -16 R_E$ (dotted curves), the pressure increases monotonically between -40 and $-10 R_E$ as does the number density. However, the temperature and the number density are positively correlated at large down-tail distances (-40 to $-30 R_E$) but are anticorrelated inside of $\sim -30 R_E$. In the central dawn half of the tail at $y = -8 R_E$ (dashed curves), the temperature and number density are anticorrelated at large down-tail distances (-40 to $-27 R_E$) but are positively correlated in the inner magnetotail (-25 to $-15 R_E$). We conclude that anomalous polytropic indices will relate moments of the non-Maxwellian distributions that develop throughout much of the magnetotail.

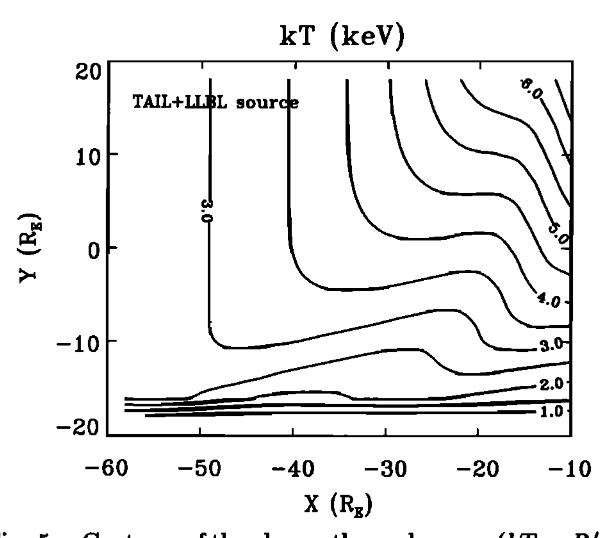

Fig. 5. Contours of the plasma thermal energy ($kT = P/n$) are shown in the magnetospheric equatorial plane for the combined deep-tail and LLBL plasma sources. The format and parameters are the same as those in Figure 2.

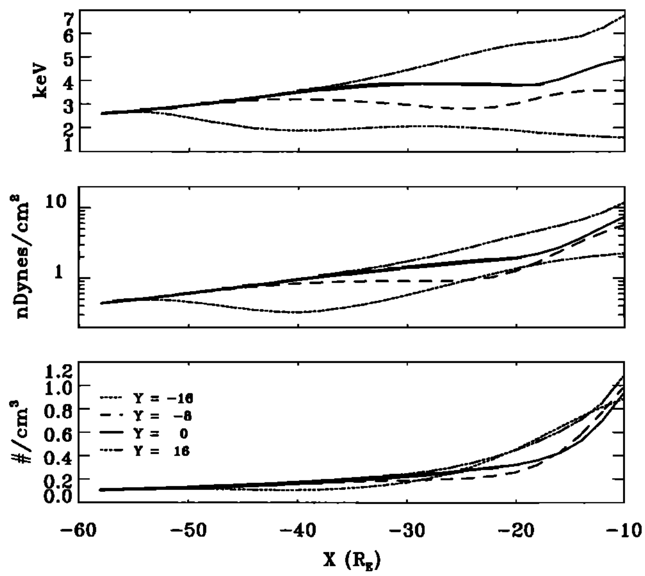

Fig. 6. Curves of the average energy, pressure, and number density of the combined plasma sources as a function of down-tail distance (x) at various fixed cross-tail (y) locations. Even with a simple two-source model, the constitutive relationship between derived bulk plasma properties is complex.

4. Summary and Discussion

We have generalized the finite tail width plasma sheet convection model to include all cross-tail equatorial locations and dual plasma sources. During periods of slow convection, a deep-tail plasma source cannot supply plasma to the entire plasma sheet; a key additional source of ions is the dawnside LLBL. This source supplies a significant portion of the pressure-carrying ions primarily near the inner edge of the plasma sheet and near the dawnside flank of the magnetotail as proposed by *Eastman et al.* [1985].

The model predicts several large-scale features in the bulk plasma properties for a slowly convecting magnetotail. Principally in the near magnetotail, the westward (cross-tail) gradient/curvature drift of ions creates a duskward plasma pressure gradient. The cross-tail pressure gradient arises primarily from an increase in the average plasma thermal energy from the dawn to the dusk magnetotail flank; the number density remains relatively uniform.

Although the model is neither complete nor quantitatively precise, we believe the qualitative effects should be present and observable at quiet times. We expect the magnitude of the cross-tail ion pressure gradient to be large (i.e., comparable to the earthward pressure gradient in this same region) when the cross-tail potential is near its minimum (15 kV).

We propose that the drift-induced pressure gradient is balanced in part by the oppositely directed magnetic pressure gradient in the plasma sheet reported by *Fairfield* [1986]. The ion pressure gradient may be partially balanced also through the effects of magnetic tension or through a time-dependent convection process.

It is worthwhile to note briefly the effects anticipated when the cross-tail electric potential is enhanced. As the potential increases (i.e., as τ increases), the inner magnetotail cross-tail pressure gradients become less significant. In addition, there is less mixing of the plasmas from the dual sources as the particles follow orbits that are more nearly aligned in the Earth-Sun direction. For instance, in Figure 2*d* we showed that at the inner boundary of the model ($x = -10$), more (less) than 50% of the particles contributing to the plasma pressure originated from the tail source for $y > 10$ ($y < 10$) for a total cross-tail potential drop of 15 kV. As the potential drop increases to 30 kV (60 kV), the equivalent demarcation moves from $y = 10$ to $y = -5$ ($y = -13$). Finally, the inward plasma pressure gradients become large as the cross-tail potential increases and could well lead to the pressure balance inconsistency that *Erickson and Wolf* [1980] proposed as a trigger of large-scale, time-dependent reconfigurations of the magnetic field and plasma. Most of the pressure increase for large cross-tail potential is due to the deep-tail plasma source rather than the LLBL plasma source. We find (see also KS88) that for $\tau_T(y_f = 0) > 5$ (or equivalently, with our assumed plasma parameters, a total cross-tail potential greater than 25 kV), the pressure-balance inconsistency develops. Therefore the conclusions reached above are limited to those geomagnetically quiet periods characterized by sufficiently slow and steady magnetospheric convection.

Several deficiencies of the model must be stressed. The role of electrons has been neglected. This means that we have not dealt with electron contributions to the plasma pressure and we have ignored problems of maintaining charge neutrality. Let us consider the ways in which these matters will affect our results. Clearly, electrons drift from dusk to dawn (eastward) across the magnetotail. Thus a dusk-to-dawn electron pressure gradient across the tail should exist. As the electron energy density is small relative to the ion energy density (on average $\sim 1/7$), the net cross-tail plasma pressure is dominated by the ions. However, an additional effect virtually removes the electron contribution to cross-tail pressure gradients in our model. Recall that the gradient is a function of τ, a parameter that must be ≤ 10 for finite width effects to be important. As source electrons are much cooler than source ions, the value of τ for electrons is ~ 7 times greater than for ions (i.e., $\tau \approx 20$ even at quiet times) meaning that for electrons the finite width tail effects are truly unimportant.

Another interesting consequence of the difference between ion and electron convection is that in the absence of other processes, the ion temperature gradients alone imply a cross-tail variation in the electron to ion temperature ratio. We do not know if such an effect is observed. *Baumjohann et al.* [1989] report that 80% of the temperature ratios in their study of the plasma sheet plasma fell in the range of $5.5 \leq T_i/T_e \leq 11$. However, their data were not sorted by cross-tail location. It is possible that the factor of 2 variations that they found can be attributed to a y-directed gradient, but this speculation has not been tested.

What about the charge separation that arises from the fact that electrons and ions drift in opposite directions across the tail? In order to achieve charge-neutrality, field-aligned currents must flow into the ionosphere. Such currents are likely to be carried by electrons from both the magnetosphere and ionosphere. The convection system is then modified by the magnetosphere-ionosphere coupling through closure currents. We have ignored this aspect of the process, but it has recently been treated extensively elsewhere [*Erickson et al.*, 1991; *Liu and Rostoker*, 1991]. *Erickson et al.* [1991] suggest that the field-aligned currents established through convection map to, and define, the Harang discontinuity. They argue further that in the magnetospheric equatorial plane the electric fields mapping from the Harang discontinuity are skewed from a uniform cross-tail orientation so as to alter the westward gradient/curvature drift effects (as suggested previously by *Atkinson* [1984]). The Harang discontinuity electric field component points approximately sunward at radial distances greater than the location of the convection reversal (i.e., at relatively higher magnetic latitudes) and antisunward inside the reversal distance. As a result, at larger distances the skewed electric field causes an $\mathbf{E}\times\mathbf{B}$ ion drift in the dusk-to-dawn direction, thereby counteracting the dawn-to-dusk gradient/curvature drift. Therefore self-consistent inclusion of magnetosphere-ionosphere coupling reduces (enhances) the magnitude of the cross-tail pressure gradient antisunward (sunward) of the reversal in the meridional magnetospheric electric field. The degree to which ionospheric coupling is important to modifying the results of our analysis, rests largely on the magnitude of the Harang discontinuity electric field and the details of the mapping of the ionospheric electric field to the magnetospheric equatorial plane. Further observational work is required to provide this information.

Finally, we reiterate that our model is time-independent and therefore applicable only for periods of very slow bulk plasma sheet convection ($\tau \leq\sim 5$). We recognize that more rapid convection requires time-dependent resolutions to the pressure-balance inconsistency, as was described originally by *Erickson and Wolf* [1980]. We also point out that our model is valid only for descriptions of the average, large-scale magnetotail convection system. Both *Baumjohann et al.* [1989] and *Angelopoulos et al.* [1992, 1993] have shown that even during magnetically quiet periods, large, bursty flows are superimposed on the overall background flow in the central plasma. These large magnitude, and possibly local, transient flows may even constitute a large fraction of the bulk transport process and therefore may negate the quasi-static approximation as an average description. However, recent studies of ion flows in the quiet time inner plasma sheet [*Angelopoulos et al.*, 1993] show that when the bursty, bulk flows are excised from the ISEE and IRM plasma flow data sets, the time-averaged background flow approximates the flow found in our model. While considerable flow variability is undoubtedly an important element of plasma sheet convection, even during quiet times, the type of global flow pattern that we have discussed appears to describe the time-averaged moments of the plasma.

The convection model described in this paper emphasizes processes that are not modeled by ideal MHD which may therefore be inapplicable for some aspects of the slowly convecting magnetotail. While the gradient/curvature drift of ions, central to the finite tail width mechanism, may be represented as heat and mass fluxes in an MHD formulation, non-Maxwellian velocity phase space distributions are not generally accounted for within magnetohydrodynamic plasma descriptions. As we have remarked, the non-Maxwellian distributions may be quite important for describing magnetotail plasma sheet convection. Therefore we have emphasized the importance of the phase space density, rather than the bulk moments of the distribution function which may mask important physical information pertaining to magnetotail particle transport. It is clear that future convection models should consider not only the kinetic effects arising from a finite energy plasma but also other associated modifications of a strictly MHD treatment.

Acknowledgments. We should like to thank G. Erickson and R. A. Wolf for many stimulating discussions and also L. Lyons and M. Schulz for helpful comments. Work performed at The Aerospace Corporation was supported by the National Aeronautics and Space Administration under grant NAGW-2126. Work performed at UCLA was supported by the National Science Foundation, Division of Atmospheric Sciences, under grant ATM 91-15557.

The Editor thanks W. W. Liu and another referee for their assistance in evaluating this paper.

REFERENCES

Angelopoulos, V., W. Baumjohann, C. F. Kennel, F. V. Coroniti, M. G. Kivelson, R. Pellat, R. J. Walker, H. Lühr, and G. Paschmann, Bursty bulk flows in the inner central plasma sheet, *J. Geophys. Res.*, *97*, 4027, 1992.

Angelopoulos, V., et al., Characteristics of ion flow in the quiet state of the inner plasma sheet, *Geophys. Res. Lett.*, in press, 1993.

Ashour-Abdalla, M., L. M. Zelyni, and J.-M. Bosqued, The formation of the wall region: Consequences in the near Earth magnetotail, *Geophys. Res. Lett.*, *19*, 1739, 1992.

Atkinson, G., Thick current sheets in the renovated model of the magnetosphere, *J. Geophys. Res.*, *89*, 8949, 1984.

Baumjohann, W., and G. Paschmann, Determination of the polytropic index in the plasma sheet, *Geophys. Res. Lett.*, *16*, 295, 1989.

Baumjohann, W., G. Paschmann, and C. A. Cattell, Average plasma properties in the central plasma sheet, *J. Geophys. Res.*, *94*, 6597, 1989.

Bevington, P. R., *Data Reduction and Error Analysis for the Physical Sciences*, pp. 212-214, McGraw-Hill, New York, 1969.

Birn, J., Magnetotail equilibrium theory: The general three-dimensional solution, *J. Geophys. Res.*, *92*, 11,101, 1987.

Eastman, T. E., L. A. Frank, and C. Y. Huang, The boundary layers as the primary transport regions of the Earth's magnetotail, *J. Geophys. Res.*, *90*, 9541, 1985.

Erickson, G. M., Modeling of plasma-sheet convection: Implications for substorms, Ph.D. dissertation, Rice Univ., Houston, Tex., 1985.

Erickson, G. M., and R. A. Wolf, Is steady state convection possible in the Earth's magnetosphere?, *Geophys. Res. Lett.*, *6*, 897, 1980.

Erickson, G. M., R. W. Spiro, and R. A. Wolf, The physics of the Harang discontinuity, *J. Geophys. Res.*, *96*, 1633, 1991.

Fairfield, D. H., The magnetic field of the equatorial magnetotail from 10 to 40 R_E, *J. Geophys. Res.*, *91*, 4238, 1986.

Goertz, C. K., and W. Baumjohann, On the thermodynamics of the plasma sheet, *J. Geophys. Res.*, *96*, 20,991, 1991.

Hau, L.-N., R. A. Wolf, G.-H. Voigt, and C. C. Wu, Steady-state magnetic field configurations for the earth's magnetotail, *J. Geophys. Res.*, *94*, 1303, 1989.

Huang, C. Y., C. K. Goertz, L. A. Frank, and G. Rostoker, Observational determination of the adiabatic index in the quiet time plasma sheet, *Geophys. Res. Lett.*, *16*, 563, 1989.

Kan, J. R., and W. Baumjohann, Isotropized magnetic-moment equation of state for the central plasma sheet, *Geophys. Res. Lett.*, *17*, 271, 1990.

Kan, J. R., W. Sun, and W. Baumjohann, A hybrid equation of state for the quasi-static central plasma sheet, *Geophys. Res. Lett.*, *19*, 421, 1992.

Kivelson, M. G., Magnetospheric electric fields and their variation with geomagnetic activity, *Rev. Geophys. Space Phys.*, *14*, 189, 1976.

Kivelson, M. G., and H. E. Spence, On the possibility of quasi-static convection in the quiet magnetotail, *Geophys. Res. Lett.*, *15*, 1541, 1988.

Liu, W. W., and G. Rostoker, Effects of dawn-dusk pressure asymmetry on convection in the central plasma sheet, *J. Geophys. Res.*, *96*, 11,501, 1991.

Pontius, D. H., and R. A. Wolf, Transient flux tubes in the terrestrial magnetosphere, *Geophys. Res. Lett.*, *17*, 49, 1990.

Pritchett, P. L., and F. V. Coroniti, Plasma sheet convection and the stability of the magnetotail, *Geophys. Res. Lett.*, *17*, 2233, 1990.

Schindler, K., and J. Birn, Magnetotail theory, *Space Sci. Rev.*, *44*, 307, 1986.

Southwood, D. J., and R. A. Wolf, An assessment of the role of precipitation in magnetospheric convection, *J. Geophys. Res.*, *83*, 5227, 1978.

Spence, H. E., and M. G. Kivelson, The variation of the plasma sheet polytropic index along the midnight meridian in a finite width magnetotail, *Geophys. Res. Lett.*, *17*, 591, 1990.

Spence, H. E., M. G. Kivelson, R. J. Walker, and D. J. McComas, Magnetospheric plasma pressures in the midnight meridian: observations from 2.5 to 35 R_E, *J. Geophys. Res.*, *94*, 5264, 1989.

Tsyganenko, N. A., Global quantitative models of the geomagnetic field in the cislunar magnetosphere for different disturbance levels, *Planet. Space Sci.*, *35*, 1347, 1987.

Walker, R. J., and T. Ogino, Global magnetohydrodynamic simulations of the magnetosphere, *IEEE Trans. Plasma Sci.*, *17*, 135, 1989.

Zhu, X. M., Plasma sheet polytropic index as inferred from the FPE measurements, *Geophys. Res. Lett.*, *17*, 2321, 1990.

Zhu, X. M., The magnetospheric convection pattern and its implications, *J. Geophys. Res.*, in press, 1993.

M. G. Kivelson, Department of Earth and Space Sciences and Institute of Geophyics and Planetary Physics, University of California, Los Angeles, CA 90024.

H. E. Spence, Space and Environment Technology Center, The Aerospace Corporation, Los Angeles, CA 90009.

(Received February 25, 1991;
revised April 7, 1993;
accepted May 20, 1993.)